Uludağ University Journal of The Faculty of Engineering, Vol. 25, No.3, 2020 RESEARCH

DOI: 10.17482/uumfd.787147

PROBABILISTIC RUNOFF MODELING APPROACH IN MOUNTAINOUS BASINS BASED ON SATELLITE SNOW DATA AND WAVELET NEURAL NETWORK

Gökçen UYSAL [*]
Aynur ŞENSOY [*]

Received: 28.08.2020; revised: 16.10.2020; accepted: 12.11.2020

Abstract: Streamflow prediction is often a challenging issue for snow dominated basins where proper in-situ snow data might be limited and the snow physics is highly complex. The main aim of this study is to propose an alternative modeling solution by considering both accessibility of the inputs and simplicity of the model structure. We propose Wavelet Neural Network (WNN) model approach which takes probabilistic snow cover area in order to produce probabilistic streamflow in the mountainous basins. For the sake of the accessibility of the input data, snow probability maps are produced from cloud-free images of MODIS. The WNN model is trained and tested with observed hydro-meteorological data. Also, Multi-Layer Perceptron Model (MLP) is used as a benchmark model. The approach is tested in a snow-dominated headwater (in altitude from 1559 to 3508 m) of Murat River which has a great importance as being one of the main tributaries of Euphrates River. According to the results, the approach is capable of detecting snow distribution in the area of interest and WNN is promising to generate probabilistic streamflow predictions.

Keywords: Snowmelt modeling, Wavelet Neural Network, Euphrates River Basin, Streamflow prediction, Satellite snow data

Dağlık Havzalarda Uydu Kar Verisi ve Dalgacık Sinir Ağı Tabanlı Olasılıklı Akım Modelleme Yaklaşımı

Öz: Kar baskın havzalardaki akarsu akım tahminleri, uygun arazi kar verilerinin sınırlı oluşu ve kar fiziğinin oldukça karmaşık olması nedeniyle genellikle zorlayıcı bir konudur. Bu çalışmanın temel amacı hem girdilerin erişilebilirliğini hem de model yapısının basitliğini göz önünde bulundurarak alternatif bir modelleme çözümü önermektir. Önerilen Dalgacık Sinir Ağı (DSA) modeli yaklaşımı, nehir akımları üretmek için olasılıklı karla kaplı alanları girdi alarak dağlık havzalarda olasılıklı akım tahminleri üretebilmektedir. Girdi verilerinin erişilebilirliği adına, MODIS'in bulutsuz görüntülerinden kar olasılığı haritaları üretilmektedir. DSA modeli, gözlenmiş hidro-meteorolojik verilerle eğitilmiş ve test edilmiştir. Ayrıca, Çok-Katmanlı Perseptron Modeli (ÇKPM) de kıyaslama modeli olarak kullanılmıştır. Yaklaşım, Fırat Nehri'nin ana kolu olarak büyük önem taşıyan Murat Nehri'nin kar baskın üst havzasında (1559 ila 3508 m yükseklikte) test edilmiştir. Sonuçlara göre, DSA yaklaşımı ilgi alanındaki kar dağılımını tespit ederek olasılıklı akım tahminleri üretme imkânı sağlamaktadır.

Anahtar Kelimeler: Kar erimesi modelleme, Dalgacık Sinir Ağı, Fırat Nehri havzası, Akım tahmini, Uydu kar verisi

[*] Eskişehir Teknik Üniversitesi, 2 Eylül Kampüsü, Mühendislik Fakültesi, İnşaat Mühendisliği, 26555, Eskişehir
İletişim Yazarı: Gökçen Uysal (gokcenuysal@eskisehir.edu.tr)

1. INTRODUCTION

Predicting snowmelt runoff necessitates estimating snow components in mountainous catchments. Observation network is rather limited in many mountainous catchments, although dense station network is advised for proper measurement (WMO, 2008). This situation accelerated the use of remote sensing techniques and satellite data in snow hydrology studies. The satellite-based monitoring and processing of snow cover are well-known techniques. Snow can be detected by optical satellites and processed in different algorithms. There are variety of satellites among which MODIS (Moderate Resolution Imaging Spectroradiometer) with visible/near infrared sensors on Terra and Aqua platforms provides processed Snow Cover Area (SCA) products since early 2000s with different spatial resolutions (Hall, et al. 2006). There are number of studies on the validation and use/application of these products in the world and in Turkey (Tekeli et al., 2005; Hall & Riggs, 2007; Parajka & Blöschl, 2008; Şorman et al., 2009; Şensoy & Uysal, 2012; Krajčí et al., 2014; Finger et al., 2015; Uysal et al., 2016). On the other hand, snow cover data does not represent the actual amount of water stored in a snowpack, therefore snow cover data is usually used together with hydrological tools to get snowmelt and/runoff depending on the purpose of applications.

The use of SCA in different hydrological applications requires a systematic and continuous mapping of snow however in general there are discontinuities in satellite data set due to various realities as the presence of cloud cover in optical microwave satellites, cost and time constraints of acquiring and processing satellite data depending on the scale of the basin. Moreover, characterization of snow dynamics may require a general overview of snow conditions in the basin. In such circumstances probabilistic analysis of satellite snow cover data based on long term time series of available satellite observations would be a beneficial data source.

Alternative to conceptual modeling approach, Artificial Neural Networks (ANN) as one of the machine learning models are sometimes preferable for solving large scale problems such as pattern recognition, nonlinear modeling, classification, association etc. Contrary to conceptual models, data-driven models require little knowledge of the physical processes modelled and rely on the data describing input and output characteristics, based on which they are able to generalize the process (Daliakopoulos & Tsanis, 2016). ANN as a multi-parameter nonlinear function that can be calibrated to simulate the behavior of a known dataset (Solomatine, 2002) can overcome practical limitations as lack of adequate historical data in ungaged or poorly gaged basins in regard to a mathematical point of view instead of physical reasoning. Different types of ANN models were applied to increase the performance of the rainfall-runoff modeling and streamflow prediction in the recent literature including snow hydrology (Daliakopoulos & Tsanis, 2016; Uysal et al., 2016; Fahimi et al., 2017). Moreover, ANNs can provide superior results when used with different memory structures and decomposition techniques. The wavelet transform is one of the powerful mathematical tools that provides both time and frequency representation of an analyzed nonlinear signal in the time domain (Daubechies, 1992). A signal can be decomposed to dilations and translations parameters, and then information in the signal is presented by these parameters in the form of frequencies (Al-geelani et al., 2012). There are several applications in literature which use WNN models to improve the modeling results such as structural system identification (Adeli et al., 2006), traffic flow modeling (Jiang et al., 2005), time-series prediction (Chen et al., 2006), groundwater level forecasting (Adamowski and Chan, 2011), river water temperature forecasting (Graf et al., 2019).

Over the last few years, probabilistic runoff forecasts have become more popular in hydrology primarily in studies that have focused on flood forecasting (Pappenberger et al., 2005; Verbunt et al., 2007; Fundel & Zappa, 2011; Ramos et al., 2013; Dale et al., 2014; Jörg-Hess et al., 2015; Şorman et al., 2019) since they have an advantage of representing the uncertainty of meteorological inputs. Moreover, snow is an essential component of hydrological cycle in mountainous regions and several studies have found that including remotely sensed snow data successfully improves probabilistic runoff predictions.

In this study we introduce probabilistic runoff modeling using the benefit of snow extent fostering on the prior data set of satellite snow cover of MODIS and data driven modeling approach with wavelet decomposition (WNN) in a relatively less studied and data sparse mountainous headwaters of Euphrates Basin. The results are also compared with a benchmark Multi-Layer Perceptron (MLP) model which represents ANN-only approach.

2. MATERIALS AND METHOD

The proposed probabilistic runoff modelling approach is comprised of two major steps:

(i) Extraction of snow maps based on probability analysis of archived satellite snow extent data,

(ii) Development of a data driven model based on neural network and wavelet decomposition making use of snow maps produced from the previous step as one of the main forcing inputs.

The approach is shown by a flow chart in Figure 1 and the details of the materials and method are described in this section.

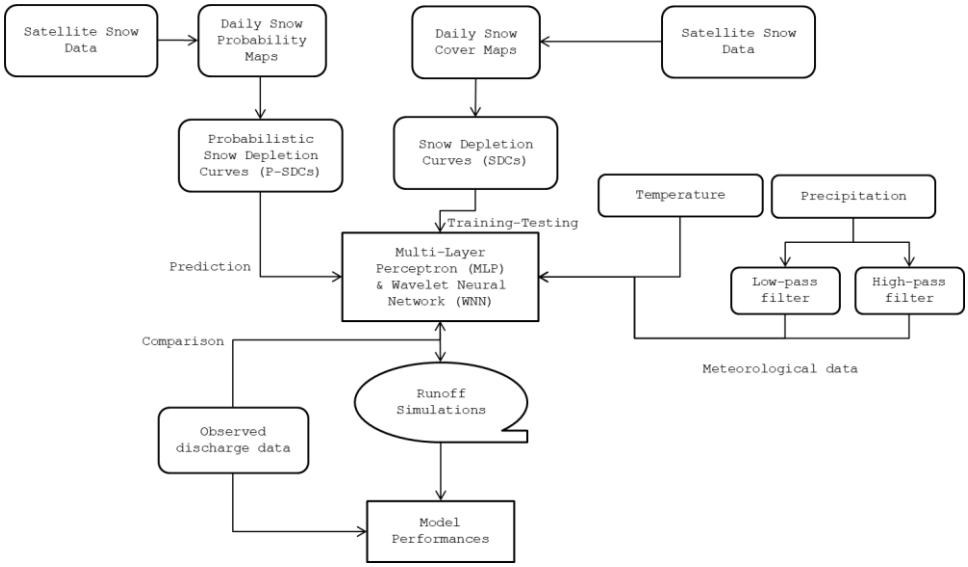

Figure 1:
Probabilistic runoff modeling schematic

2.1. Study Area

Modeling the amount and timing of runoff at the headwaters of Euphrates River has great importance for the operation of downstream reservoirs in the Eastern Anatolia, Turkey. The Upper Murat Basin (hereinafter, Murat Basin) located in the upper part of Murat River Basin having the drainage area of 40,000 km^2. The study basin lies within the longitudes 42^o 00’ E to 43^o 50’ E and latitudes 39^o 10’ N to 40^o 00’ N. It has a drainage area of 5,910 km^2 and its elevation ranges in altitude from 1559 to 3508 m. The main land cover types are pasture (32.6%), agriculture (36.1%), bareland (30.8%) and the others (urban, forest, lakes etc., 0.6%). The location and elevation ranges of Murat Basin along with the observation network are provided in Figure 2. Murat Basin is controlled by stream gauging station of E21A022 at Tutak location. Table 1 describes a summary of basin topographic properties.

Since the topography is rough, the catchment has a scarce observation network. There is only one meteorological station (Agri at 1632 m) to record daily precipitation (P) and temperature (T)

in the catchment as shown in Figure 2. In this study, a year period is defined as a water-year concept that starts at 1st of October of the previous year and ends on 30th September of the current year. Average annual precipitation and temperature values are 522 mm and 6.2 ^{0}C, respectively, for the long-term records. The variation of annual average P and T values along with the years are shown in Figure 3 for the period of probabilistic snow extent analysis. Discharge data is available for the water-years of 2001-2013 and 2015 (2014-water year streamflow data is missing).

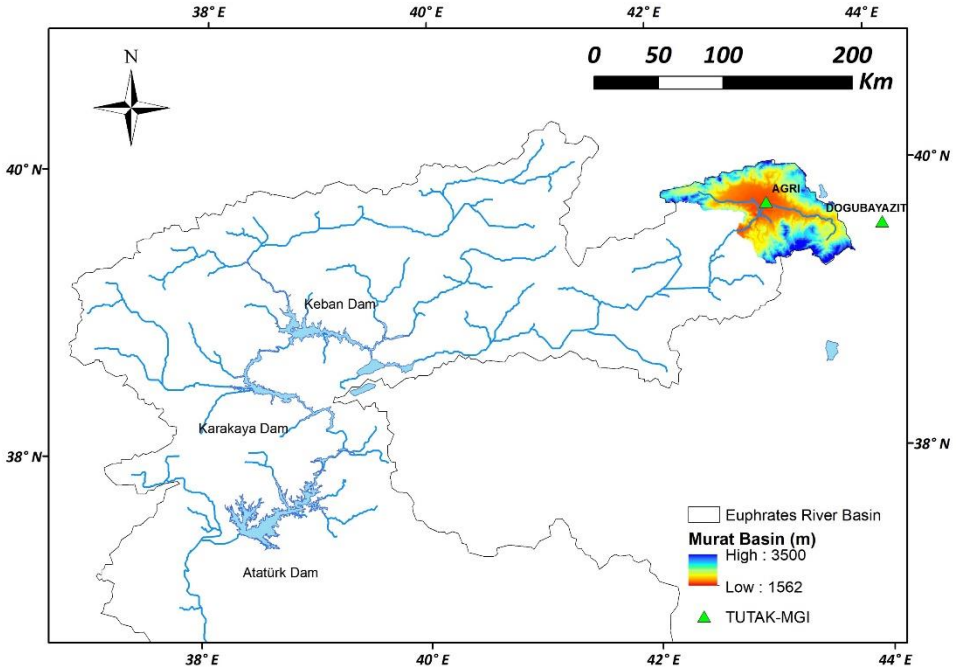

Figure 2:
Location, digital elevation model and the observation network of The Upper Murat Basin

Table 1. Topographic properties of the basin

Zone	Elevation Range (m)	Area (km^2)	Area (%)	Hypsometric mean elevation (m)
A	-	-	-	-
B	1559-1900	1762	29.8	1725
C	1900-2300	2205	37.3	2100
D	2300-2900	1779	30.1	2475
E	2900-3508	166	2.8	3080
Whole catchment	1559-3508	5912	100.0	2125

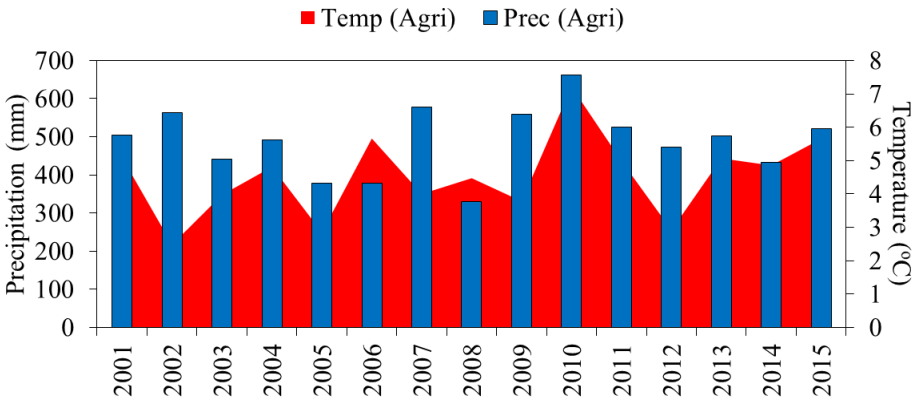

Figure 3:
Average annual precipitation and temperature records of Agri station

2.2. Satellite snow cover data

MOD10A1 (Terra) and MYD10A1 (Aqua) products are being produced and distributed by the NASA Distributed Active Archive Center (DAAC) located at the National Snow and Ice Data Center (NSIDC). MODIS Reprojection Tools is used to tile the images. The tiled images were then reprojected to World Geodetic System 1984 (WGS84), Universal Transverse Mercator (UTM) Zone 37 with a cell size of 500 m.

The MODIS snow-mapping algorithm is fully automated and is based on the Normalized Difference Snow Index (NDSI) with a set of thresholds (Hall et al., 2002). Based on NDSI and threshold values, snow cover pixels are separated from non-snowy areas using Eq. (1).

$$NDSI = \frac{MODIS_{B4} - MODIS_{B6}}{MODIS_{B4} + MODIS_{B6}} \tag{1}$$

Depletion of snow is revealed in terms of percentage of the snow cover area along with a time horizon for each time period (mainly day, or sometimes 7-days).

2.3. Snow probability maps

Probability of snow occurrence is calculated using daily SCA images and pixels are classified as snow, no snow and cloud (including undetermined pixels). Then, each SCA image is reclassified such that snow or cloud observations are equal to one, and all other attributes are equal to zero to derive a probability map. Probability of snow for a pixel is calculated as:

$$P_{(t)} = \frac{\sum_{i=1}^{n} S_{(t,i)}}{n - \sum_{i=1}^{n} C_{(t,i)}} \tag{2}$$

where t stands for day, S and C stands for observations of snow and cloud, respectively, n stands for the total observation period in years.

Optical satellites suffer from cloud coverage and therefore images are pre-processed before to be used in the probability analysis. Filtering process (such as temporal, spatial, elevation) is used to remove cloud cover from the images (Şorman & Yamankurt, 2011). Since the method is capable of eliminating cloud cover and can provide binary snow/no snow areas, Equation 2 is updated with no cloud component in the denominator.

2.4. Wavelet neural network (WNN) model

Artificial Neural Network (ANN) has been developed based on the inspiration of biological neural network of the human brain. Basically, it is characterized by its architecture that represents the pattern of connection between nodes, method of determining the connection weights, and the activation function (Haykins, 2009). Multi-Layer Perceptron (MLP) is a form of feedforward network that has interconnected neurons arranged into three layers: input layer, a hidden layer and an output layer and uses backpropagation algorithm in the training stage. Moreover, MLP-ANN models are the most applied ANN types in hydrology field (Maier & Dandy, 2000; Zhao et al., 2005; Maier et al., 2010). A node is a processor, which is connected to the others by weights, whereas the nodes are generally arranged in layers. The output of an individual neuron (weighted sum of all its inputs), is obtained by the following equation:

$$Ny_j = f\left(\sum_{i=0}^{n}\left(w_{ij}x_i - b_{ij}\right)\right) \tag{3}$$

where, $x_i = (x_1, \dots, x_i, \dots, x_n)$ and $w_{ij} = \left(w_{1j}, \dots, w_{ij}, \dots, w_{nj}\right)$, x_i is the information from previous nodes, w_{ij} represents the connection weight from the i^{th} node in the preceding layer to this node, where b_{ij} is the bias, f is the activation function.

Activation function may be linear, threshold, logistic sigmoid, Gaussian or hyperbolic tangent functions depending on type of the network and training algorithm used in the application. Mainly sigmoid functions are used in rainfall-runoff processes due to having bounded, monotonic, nondecreasing function that provides a graded, nonlinear response (ASCE, 2000). In this study, sigmoid function is used for the hidden layer and linear transfer function is used for the output layer. It is recommended to employ data preprocess (inputs and outputs) to have better performance before training. Normalization eliminates sensitivity of the network for different range of inputs. Considering that, firstly all inputs and outputs are normalized between [0.1 – 0.9] using Equation 4:

$$X = \frac{x_i - x_{min}}{x_{max} - x_{min}} \tag{4}$$

where, X stands for standardized data vector, x_{min} and x_{max} are minimum and maximum values of the data set.

In this study, different than conventional MLP, two filters (i.e., low-pass filter and high-pass filter) are used to decompose the original data series (here, some selected input vectors) into the approximation and detailed subseries. 1-D wavelet decomposition is employed to perform a single-level wavelet decomposition of input signals using wavelet family of ‘db1’. The names of the Daubechies family wavelets are written dbN, where N is the order, and db the "surname" of the wavelet. Db1 also known as the Haar wavelet is the only orthogonal wavelet with linear phase. The original time series is passed through high-pass and low-pass filters, and detailed coefficients (cD1) and approximation coefficients (cA1) are obtained in Discrete Wavelet Transform (DWT). Wavelet Neural Network (WNN), which is employed in this study, refers to rainfall-runoff relationship by combining MLP and DWT (Figure 4). Besides, a MLP model that represents ANN-only approach is used as a benchmark model. The models are coded using MATLAB (R2019b, License number: 991708).

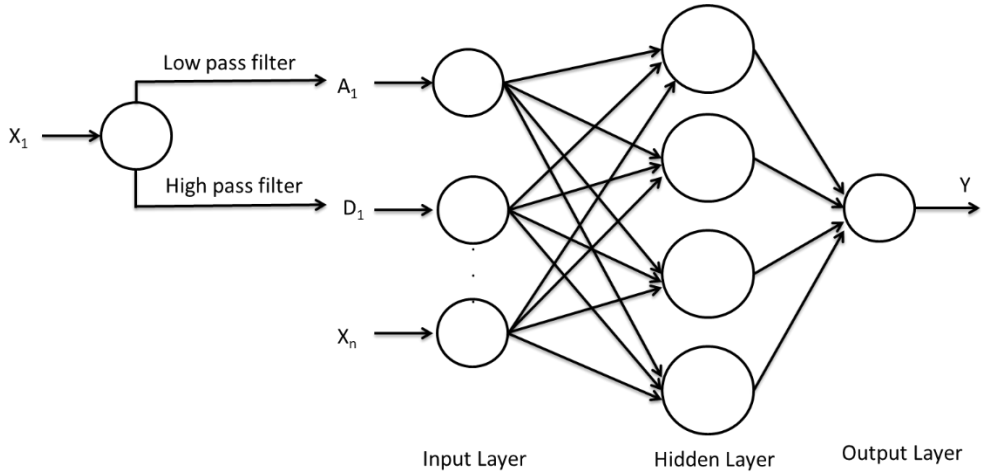

Figure 4:
Schematization of the WNN Model ($X_1 \ldots X_n$ stands for 1 to n number of input variables, A_1 and D_1 stand for the approximation member and the detailed member of input variable X_1, respectively and Y stands for the output variable)

MLP feedforward networks use gradient based training algorithms. In general, second-order nonlinear optimization techniques are usually faster and more reliable. Thus, model is trained using a well-known Levenberg-Marquart technique (Hagan & Menhaj, 1994) as it is more powerful than the conventional gradient techniques. The training is accomplished according to the weight update equation which takes the following general form as (Parisi et al., 1996):

$$w_{n+1} = w_n - [H + \lambda]^{-1} \nabla_{wn} \mathrm{E} \tag{5}$$

where, w_{n+1} and w_n are weights at $(n+1)^{th}$ and n^{th} pass (epoch), $H = J^T J$, where J is Jacobian matrix, λ is momentum, $\nabla_{wn}\mathrm{E}$ is equal to the negative of the gradient error, E is learning rate (avoids the training being trapped in a local minima instead of global minima).

Care must be taken to the generalization of the network for a given problem. Therefore, it is very vital to prevent the network that of over familiarized with the calibration data set. In this study, the training is stopped according to cross-validation using an independent test set. To that end, 15% data are randomly selected from training set and training is stopped according to cross-validation error. Since a generic method to estimate the model structure is not available, most of them rely on trial and error approach. The network architectures (models) are derived similarly by changing the network and analyzing the results in terms of error. It is also not desired to have complex networks if one with less neuron and inputs give similar results. In this study, hydro-meteorological data records are provided from an automated weather and flow measurement station. Six hidden neurons are used in one single hidden layer. The network formulation is defined below:

$$Q_{(n)} = m(DP_{(n)}, AP_{(n)}, T_{(n)}, SCA_{(n)}) \tag{6}$$

where, Q, m , DP , AP , T , SCA and n stands for streamflow [m^3/s], neural network model, detailed member for total precipitation [mm], approximation member for total precipitation [mm], air temperature [^oC], snow cover area [%] and time index, respectively.

For the accuracy assessment, the model is tested with 4 goodness of fit criteria defined as the coefficient of determination (R^2), Nash-Sutcliffe Model Efficiency (NSE), Root Mean Square Error (RMSE), Mean Absolute Error (MAE) as denoted in equation 7-10:

$$R^2 = \left[\frac{\sum_{t=1}^{n}(Q_m^t - \overline{Q}_m)(Q_o^t - \overline{Q}_o)}{\sqrt{\sum_{t=1}^{n}(Q_m^t - \overline{Q}_m)^2}\sqrt{\sum_{t=1}^{n}(Q_o^t - \overline{Q}_o)^2}} \right]^2 \quad (7)$$

$$NSE = 1 - \frac{\sum_{t=1}^{n}(Q_o^t - Q_m^t)^2}{\sum_{t=1}^{n}\left(Q_o^t - \overline{Q}_o\right)^2} \quad (8)$$

$$RMSE = \sqrt{\frac{\sum_{t=1}^{n}(Q_m^t - Q_o^t)^2}{n}} \quad (9)$$

$$MAE = \frac{\sum_{t=1}^{n}|Q_o^t - Q_m^t|}{n} \quad (10)$$

where, Q_m^t is modelled flows, Q_o^t is observed flows, $\bar{Q}_m$ is average modelled flows, $\bar{Q}_o$ is average observed flows, n is the number of data sets.

2.5. Derivation of probabilistic snow depletion curves and employment in rainfall-runoff models

The rainfall-runoff models are trained and tested using 12 years of observed daily MODIS snow cover area percentage time-series (also known as snow depletion curves) together with meteorological data sets. Snow Probability Map (SPM) for each day is derived using that of achieved 12 years data as explained in Section 2.3. These maps show the probability of snow occurrence in each pixel having 500 m cell resolution within the study area. Later, daily maps are classified into six different classes (0, 0-0.25, 0.26-0.50, 0.51-0.75, 0.76-0.99 and 1). Reclassified probability SCA percentages (P-SCA) are calculated for each day in between 15 January – 30 June (mainly from full snow cover to no-snow period). Probabilistic time series data (also called as probabilistic depletion curves, P-SDC) sets are generated using P-SCA values for each class. Finally, P-SDCs are directly used in streamflow prediction part (2013-2015) which is not included in the derivation of probability maps.

3. RESULTS AND DISCUSSIONS

3.1. Snow probability maps and extensive analyses

SPMs of Murat Basin are presented for 15-day time interval in Figure 5. Snow cover considerably dominates the catchment until mid-March with high probability. Topographic variation of snow cover that indicates the changes with respect to elevation, aspect, and slope is a well-known analysis. Instead of the conventional snow cover maps, probabilistic snow cover is evaluated to understand the characteristics of topographic variation in this area. The spatial pattern of probabilistic snow cover is represented by elevation zones. The P-SCAs are derived for the selected probabilities during the snowmelt season in Figure 6. Snow disappears in the lowest zone first and highest zone last as expected. Results prove that elevation is an important factor that should be considered during snow cover analysis in any probability class. The elevation Zone-C

has similar values with that of basin average since it represents the hypsometric elevation of the basin.

Snow depletion analysis (P-SDCs) is carried out with probabilistic snow cover values (Figure 7). The lowest probability of snow on average basin scale indicates limited number of days with full snow coverage before melting besides an early and relatively sharp melting starting with the Mid-Feb; the highest probability of snow, however, shows extended accumulation period with full coverage till mid-April and then relatively slow melting pattern lasting almost to the end of June.

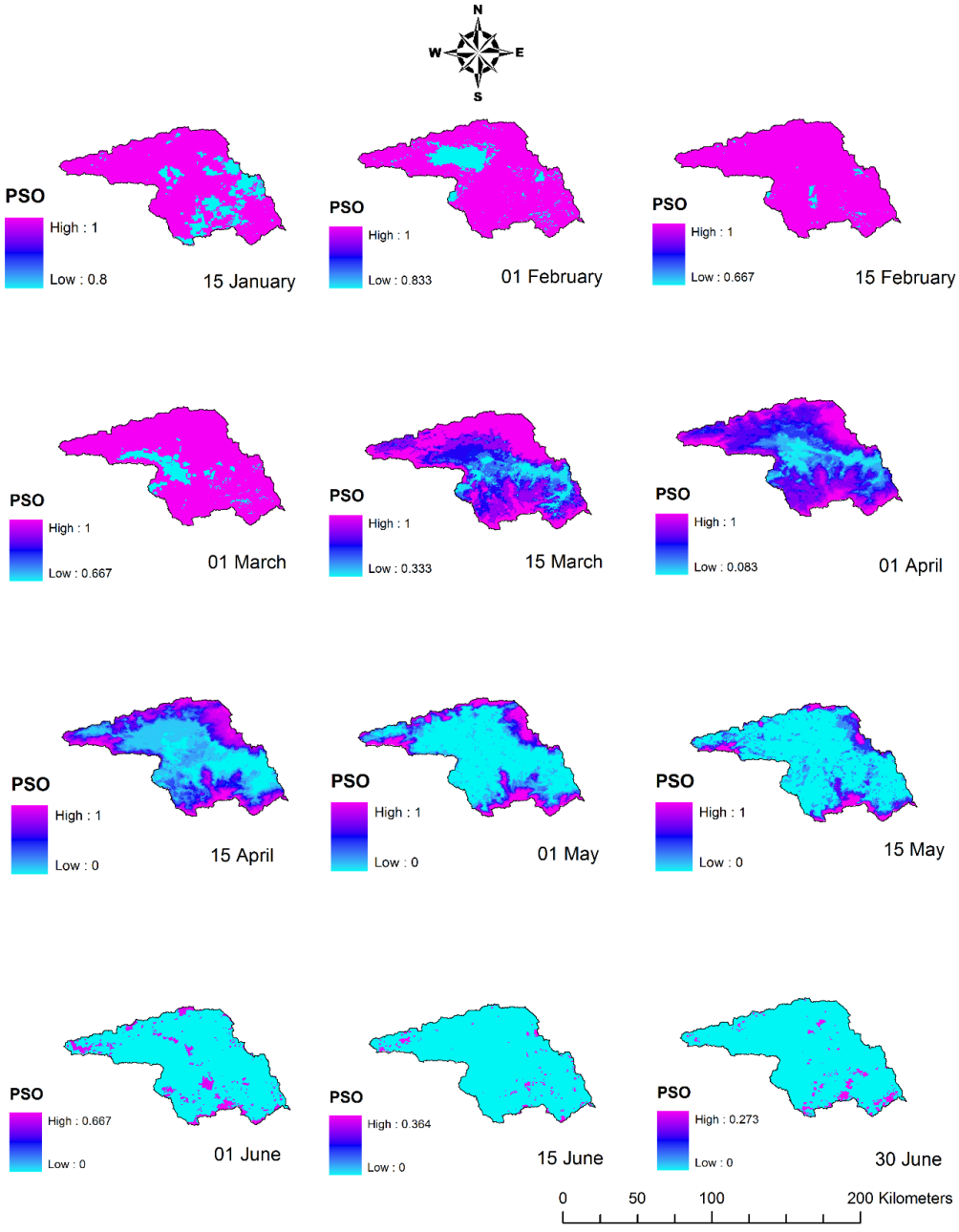

Figure 5:
Snow probability maps of Murat Basin for various dates (in between analysis period of 15 January – 30 June, PSO: probability of snow occurrence)

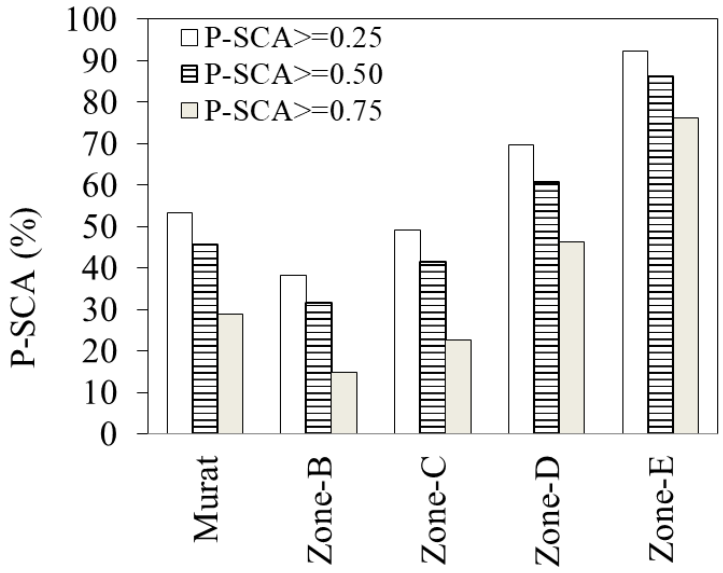

Figure 6:
Variation of P-SCA with respect to different elevation zone

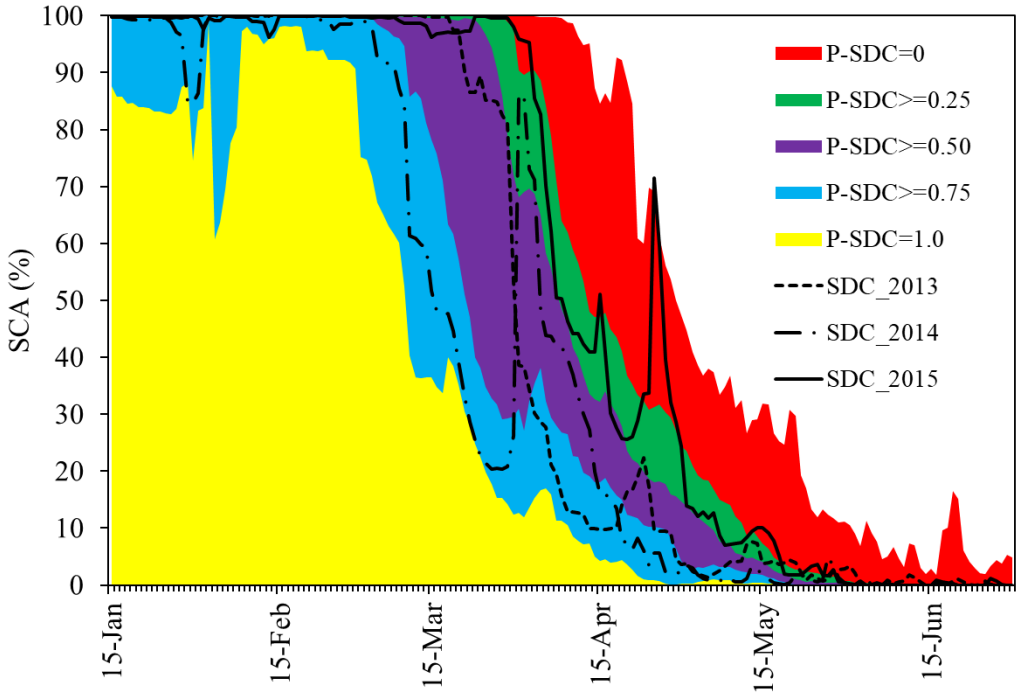

Figure 7:
Probabilistic snow depletion curves (P-SDCs) of Murat Basin with respect to different probability classes and observed snow depletion curves (SDCs)

3.2. WNN model results of the training and testing periods

The WNN model is trained and tested in 2002-2008 and 2009-2012 water years, respectively, with relatively high model performance against MLP model in such a mountainous basin as shown in Figure 8 and Table 2. The calculated performances ensure an acceptable model by

having NSE above 0.65 (Ritter & Muñoz-Carpena, 2013). MAE values are similar whereas RMSE increases in training part due to one outlier peak observed at 2004. This peak presents a real case according to the other downstream gauge.

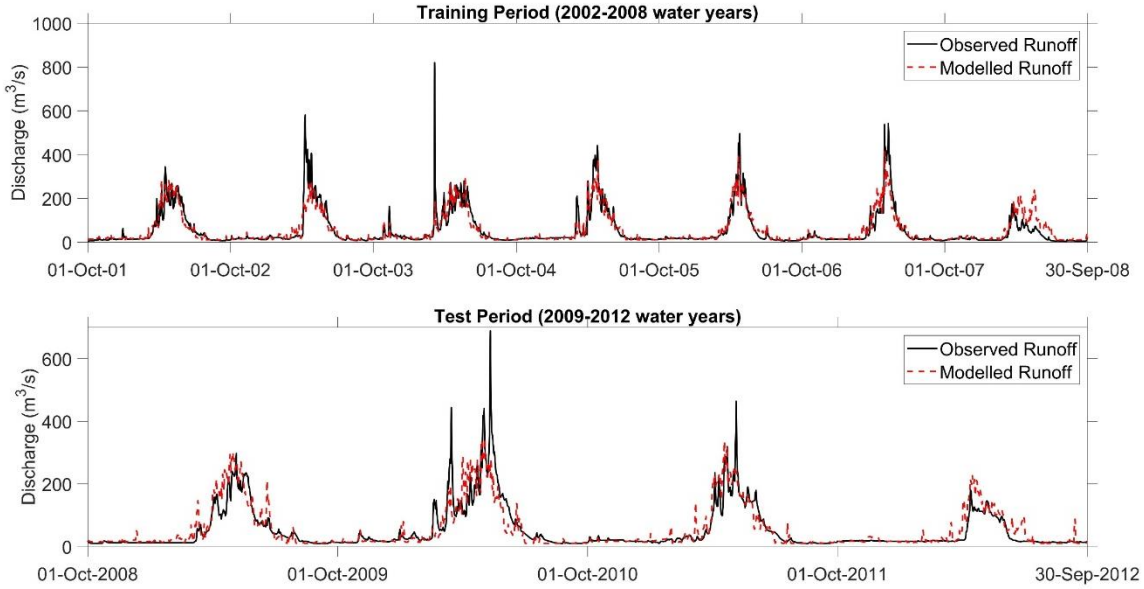

Figure 8:
Runoff predictions for training and testing periods (WNN model)

Table 2. Hydrological modeling performance

Performance criteria	Model	R^2	NSE	RMSE (m^3/s)	MAE (m^3/s)
Training period	MLP	0.68	0.68	46.5	24.0
	WNN	0.75	0.75	41.0	18.7
Testing period	MLP	0.68	0.67	40.3	21.9
	WNN	0.74	0.72	37.0	18.5

3.3. Probabilistic runoff model results model results of the training and testing periods

The developed and tested MLP and WNN models are regarded as prediction tool in this part. 2013 – 2015 which are not used in any part of training and testing is selected as the prediction period for streamflow. These years are also excluded from P-SDC analyses as well. It is important to note that 2014-water year streamflow data is missing due to technical data loss. The daily streamflow values are predicted using P-SDC data sets together with perfect prediction data. However, for the sake of a continuous model 2014 runoff values are still predicted but the performances with respect to observed discharge are given for two years (2013 and 2015). The WNN model results (P-SDC based streamflow predictions) are compared with observed discharge Figure 9. The models are also employed with observed SCA (from MODIS) for the same period and its results are denoted as "MODIS-SDC". The statistical metrics for both models (WNN and MLP) for different scenarios are given in Table 3 and Table 4. For this experiment

only P>0.25, P>0.50 and P>0.75 classes are taken into account because of P>0 (overestimates by capturing all snow-covered pixels) and P=1.0 (underestimates by capturing very few snow covered pixels) represents very unusual conditions. This experiment indicates the capability of the model with purely observed satellite data in contrast to P-SDCs. According to performances, it can be stated that QP50 and QP75 (stands for P-SDC≥0.50 and P-SDC≥0.75) present a notable performance metric in comparison with MODIS-SDC modelling result.

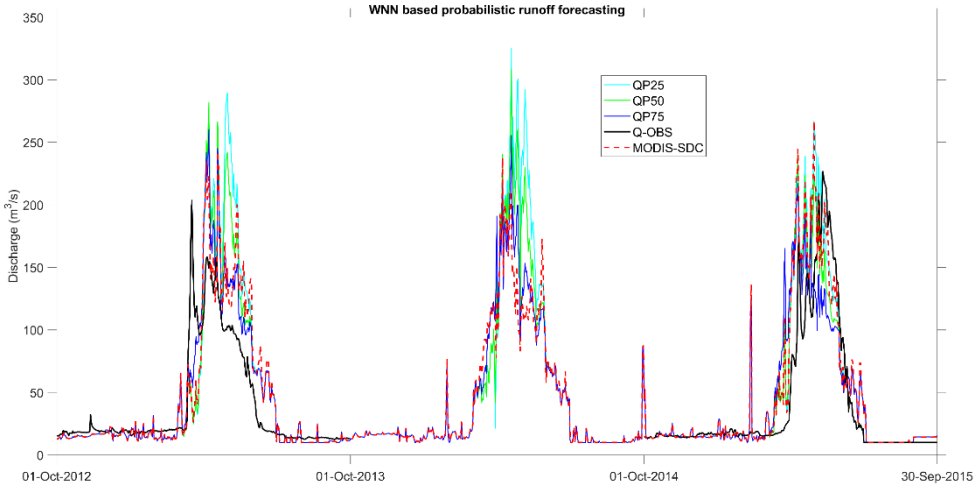

Figure 9:
Probabilistic runoff estimation for the water years of 2013, 2014, 2015 (WNN model)

Table 3. MLP modeling performances for the water years of 2013 and 2015

Scenario	R^2	NSE	RMSE (m^3/s)	MAE (m^3/s)
MODIS-SDC	0.62	0.38	36.9	25.7
QP25	0.60	0.52	38.4	26.5
QP50	0.59	0.50	39.0	27.1
QP75	0.54	0.42	44.0	29.3

Table 4. WNN modeling performances for the water years of 2013 and 2015

Scenario	R^2	NSE	RMSE (m^3/s)	MAE (m^3/s)
MODIS-SDC	0.73	0.58	30.4	16.1
QP25	0.70	0.66	38.0	19.4
QP50	0.68	0.66	34.1	18.1
QP75	0.67	0.65	30.1	16.3

4. CONCLUSION

This study attempts to find alternative and practical approaches to predict runoff in a probabilistic sense for a data scarce poorly gauged mountainous catchment. Remote sensing data sets gathered from satellite are useful but not always available for several reasons. Making use of relatively long data records of satellite snow extent, snow cover dynamics are evaluated as daily probabilistic snow cover maps. Then these snow cover maps are converted to probabilistic snow depletion curves to indicate snow covered area percentages as time-series for several probability classes. A data driven method enhanced with wavelet analysis is preferred to be coupled with satellite data. Also, a benchmark model (multi-layer perceptron) which stands for a conventional neural network model is employed and the results are compared with the proposed WNN model. Several metrics such as coefficient of determination, Nash-Sutcliffe model efficiency, root mean square error and mean absolute error are used to quantify the performances. The method is trained and tested with relatively high model performances and then probabilistic runoff predictions are obtained and compared with observed data. According to prediction scenarios, the suggested approach provides probabilistic runoff predictions in a range consisted with observed values of runoff. The study shows that the probabilistic snow cover maps derived from satellite data can be used as a valuable data source with spatial and temporal coverage for such a data scarce region. Moreover, they can directly be utilized in a data driven modeling for short or medium range ensemble runoff forecasts in a probabilistic sense when coupled with numerical weather prediction data.

ACKNOWLEDGEMENT

This study was partly funded by TÜBİTAK (The Scientific and Technical Research Council of Turkey) (Project No: 113Y075). The authors wish to thank General Directorate of Meteorology (MGM) and State Hydraulic Works (DSI) for data contribution.

REFERENCES

1. Adamowski, J., Chan, H.F. (2011) A wavelet neural network conjunction model for groundwater level forecasting. *Journal of Hydrology*, 407(1-4), 28-40. doi:10.1016/j.jhydrol.2011.06.013

2. Adeli, H., Jiang, X. (2006) Dynamic fuzzy wavelet neural network model for structural system identification. *Journal of Structural Engineering*, 132(1), 102-111. doi: 10.1061/(ASCE)0733-9445(2006)132:1(102)

3. Al-geelani, N.A., Piah, M.A.M., Shaddad, R.Q. (2012) Characterization of acoustic signals due to surface discharges on HV glass insulators using wavelet radial basis function neural networks, *Applied Soft Computing*, 12(4), 1239-1246. doi:10.1016/j.asoc.2011.12.018

4. ASCE Task Committee on Application of Artificial Neural Networks in Hydrology. (2000) Artificial neural networks in hydrology. I: Preliminary concepts, *Journal of Hydrologic Engineering*, 5(2), 115-123. doi:10.1061/(ASCE)1084-0699(2000)5:2(115)

5. Chen, Y., Yang, B., Dong, J. (2006). Time-series prediction using a local linear wavelet neural network. *Neurocomputing*, 69(4-6), 449-465. doi:10.1016/j.neucom.2005.02.006

6. Dale, M., Wicks, J., Mylne, K., Pappenberger, F., Laeger, S., Taylor, S. (2014) Probabilistic flood forecasting and decision-making: an innovative risk-based approach, *Natural Hazards*, 70(1), 159-172. doi:10.1007/s11069-012-0483-z

7. Daliakopoulos, I.N., Tsanis, I.K. (2016) Comparison of an artificial neural network and a conceptual rainfall–runoff model in the simulation of ephemeral streamflow, *Hydrological Sciences Journal*, 61(15), 2763-2774. doi:10.1080/02626667.2016.1154151

8. Daubechies, I. (1992) *Ten lectures on wavelets*. Society for Industrial and Applied Mathematics, Philadelphia, Pennsylvania.

9. Jiang, X., Adeli, H. (2005) Dynamic wavelet neural network model for traffic flow forecasting. *Journal of Transportation Engineering*, 131(10), 771-779. doi:10.1061/(ASCE)0733-947X(2005)131:10(771)

10. Graf, R., Zhu, S., Sivakumar, B. (2019) Forecasting river water temperature time series using a wavelet–neural network hybrid modelling approach. *Journal of Hydrology*, 578, 124115. doi:10.1016/j.jhydrol.2019.124115

11. Fahimi, F., Yaseen, Z.M., El-shafie, A. (2017) Application of soft computing based hybrid models in hydrological variables modeling: a comprehensive review, *Theoretical and Applied Climatology*, 128(3-4), 875-903. doi: 10.1007/s00704-016-1735-8

12. Finger, D., Vis, M., Huss, M., Seibert, J. (2015) The value of multiple data set calibration versus model complexity for improving the performance of hydrological models in mountain catchments, *Water Resources Research*, 51(4), 1939–1958. doi:10.1002/2014WR015712

13. Fundel, F., Zappa, M. (2011) Hydrological ensemble forecasting in mesoscale catchments: Sensitivity to initial conditions and value of reforecasts, *Water Resources Research*, 47(9), W09520. doi:10.1029/2010WR009996

14. Hagan, M.T., Menhaj, M.B. (1994) Training feedforward networks with the Marquardt algorithm, *IEEE Transactions on Neural Networks*, 5(6), 989-993. doi:10.1109/72.329697

15. Hall, D.K., Riggs, G.A., Salomonson, V.V., DiGirolamo, N.E., Bayr, K.J. (2002) MODIS snow-cover products, *Remote Sensing of Environment*, 83(1-2), 181-194. doi:10.1016/S0034-4257(02)00095-0

16. Hall, D.K., Riggs, G.A., Salomonson, V.V. (2006) MODIS snow and sea ice products. Editors: Qu JJ, Gao W, Kafatos M, Murphy RE, Salomonson VV. Earth Science Satellite Remote Sensing, 154-181, Springer-Verlag Press, Berlin, Heidelberg, Germany.

17. Hall, D.K., Riggs, G.A. (2007) Accuracy assessment of the MODIS snow products, *Hydrological Processes*, 21(12), 1534-1547. doi:10.1002/hyp.6715

18. Haykins, S. (2009) *Neural Networks and Learning Machines*. 3rd Ed., Pearson Prentice Hall USA.

19. Jörg-Hess, S., Griessinger, N., Zappa, M. (2015) Probabilistic forecasts of snow water equivalent and runoff in mountainous areas, *Journal of Hydrometeorology*, 16(5), 2169-2186. doi:10.1175/JHM-D-14-0193.1

20. Krajčí, P., Holko, L., Perdigão, R.A., Parajka, J. (2014) Estimation of regional snowline elevation (RSLE) from MODIS images for seasonally snow covered mountain basins, *Journal of Hydrology*, 519, 1769–1778. doi:10.1016/j.jhydrol.2014.08.064

21. Maier, H.R., Dandy, G.C. (2000) Neural networks for the prediction and forecasting of water resources variables: a review of modelling issues and applications, *Environmental Modelling & Software*, 15(1), 101-124. doi:10.1016/S1364-8152(99)00007-9

22. Maier, H.R., Jain, A., Dandy, G.C., Sudheer, K.P. (2010) Methods used for the development of neural networks for the prediction of water resource variables in river systems: Current

status and future directions, *Environmental Modelling & Software*, 25(8), 891-909. doi:10.1016/j.envsoft.2010.02.003

23. Pappenberger, F., Beven, K.J., Hunter, N.M., Bates, P.D., Gouweleeuw, B.T., Thielen, J., De Roo, A.P.J. (2005) Cascading model uncertainty from medium range weather forecasts (10 days) through a rainfall-runoff model to flood inundation predictions within the European Flood Forecasting System (EFFS), *Hydrology & Earth System Sciences*, 9, 381–393. doi:10.5194/hess-9-381-2005

24. Parajka, J., Blöschl, G. (2008) The value of MODIS snow cover data in validating and calibrating conceptual hydrologic models, *Journal of Hydrology*, 358(3-4), 240-258. doi:10.1016/j.jhydrol.2008.06.006

25. Parisi, R., Di Claudio, E.D., Orlandi, G., Rao, B.D. (1996) A generalized learning paradigm exploiting the structure of feedforward neural networks, *IEEE Transactions on Neural Networks*, 7(6), 1450-1460. doi:10.1109/72.548172

26. Ramos, M.H., van Andel, S.J., Pappenberger, F. (2013) Do probabilistic forecasts lead to better decisions?, *Hydrology & Earth System Sciences*, 17, 2219–2232. doi:10.5194/hess-17-2219-2013

27. Ritter, A., Muñoz-Carpena, R. (2013) Performance evaluation of hydrological models: Statistical significance for reducing subjectivity in goodness-of-fit assessments, *Journal of Hydrology*, 480, 33-45. doi:10.1016/j.jhydrol.2012.12.004

28. Solomatine, D.P. (2002) Data-driven modelling: paradigm, methods, experiences, *5th International Conference on Hydroinformatics*, 01-05 July, Cardiff, United Kingdom.

29. Şensoy, A., Uysal, G. (2012) The value of snow depletion forecasting methods towards operational snowmelt runoff estimation using MODIS and Numerical Weather Prediction Data, *Water Resources Management*, 26(12), 3415-3440. doi:10.1007/s11269-012-0079-0

30. Şorman, A.A., Şensoy, A., Tekeli, A.E., Şorman, A.Ü., Akyürek, Z. (2009) Modelling and forecasting snowmelt runoff process using the HBV model in the eastern part of Turkey, *Hydrological Processes*, 23(7), 1031-1040. doi:10.1002/hyp.7204

31. Şorman, A.A., Uysal, G., Şensoy, A. (2019) Probabilistic snow cover and ensemble streamflow estimations in the Upper Euphrates Basin, *Journal of Hydrology and Hydromechanics*, 67(1), 82-92. doi:10.2478/johh-2018-0025

32. Şorman, A.A., Yamankurt, E. (2011) Modified satellite products on snow covered area in upper Euphrates basin, Turkey, *European Geosciences Union General Assembly 2011*, 03 – 08 April, Vienna, Austria.

33. Tekeli, A.E., Akyürek, Z., Şorman, A.A., Şensoy, A., Şorman, A.Ü. (2005) Using MODIS snow cover maps in modeling snowmelt runoff process in the eastern part of Turkey, *Remote Sensing of Environment*, 97(2), 216-230. doi:10.1016/j.rse.2005.03.013

34. Uysal, G., Şensoy, A., Şorman, A.A. (2016) Improving daily streamflow forecasts in mountainous Upper Euphrates basin by multi-layer perceptron model with satellite snow products, *Journal of Hydrology*, 543, 630-650. doi:10.1016/j.jhydrol.2016.10.037

35. Verbunt, M., Walser, A., Gurtz, J., Montani, A., Schär, C. (2007) Probabilistic flood forecasting with a limited-area ensemble prediction system: Selected case studies, *Journal of Hydrometeorology*, 8(4), 897-909. doi:0.1175/JHM594.1

36. World Meteorological Organization (2008) Guide to Hydrological Practices. Volume I: Hydrology–From Measurement to Hydrological Information, WMO-No. 168, Geneva, Switzerland.

37. Zhao, Y., Taylor, J.S., Chellam, S. (2005) Predicting RO/NF water quality by modified solution diffusion model and artificial neural networks, *Journal of Membrane Science*, 263(1-2), 38-46. doi:10.1016/j.memsci.2005.04.004